1986

Interfacial stability of immiscible displacement in a porous medium

J. P. Stokes

D. A. Weitz

Jerry P. Gollub
Haverford College

A. Dougherty
Haverford College

Interfacial Stability of Immiscible Displacement in a Porous Medium

J. P. Stokes,[1] D. A. Weitz,[1] J. P. Gollub,[2,3] A. Dougherty,[2,3] M. O. Robbins,[4] P. M. Chaikin,[1,3] and H. M. Lindsay[1]

[1] *Exxon Research and Engineering, Annandale, New Jersey 08801*
[2] *Department of Physics, Haverford College, Haverford, Pennsylvania 19041*
[3] *Department of Physics, University of Pennsylvania, Philadelphia, Pennsylvania 19104*
[4] *Department of Physics, Johns Hopkins University, Baltimore, Maryland 21218*

(Received 7 July 1986)

We study patterns formed by the viscous fingering instability in a porous medium. The wetting properties of the medium have a profound influence on the width of the individual fingers and consequently on the shape of the overall pattern. If the displaced fluid preferentially wets the medium, the finger width is comparable to the pore size, independent of other parameters. In contrast, if the displacing fluid preferentially wets the medium, the finger width is much larger than the pore size, and, when normalized by the square root of the permeability, is found to scale with the capillary number approximately as $N_{Ca}^{-1/2}$.

PACS numbers: 47.55.Mh, 47.20.−k, 47.55.Kf

The instability that occurs when a fluid of low viscosity displaces one of higher viscosity leads to a rich variety of interfacial patterns. The simplest situation is that of the flow in a thin layer (Hele-Shaw cell), where even basic issues of hydrodynamic stability have proven surprisingly difficult to resolve, though there has been considerable recent progress.[1-7] A related but distinct problem is that of fluid displacement in a porous medium.[8-14] Both cases can be described as viscous flow governed by Darcy's law. The velocity is determined by the pressure field which is a solution to Laplace's equation, and viscous fingering instabilities occur. However, the assumption that Hele-Shaw flow provides a good model for the more complex flow in a porous medium is clearly imperfect, as is implied by the results of several recent experiments.

One of the difficulties in achieving a rigorous understanding of fluid displacement in porous media is the large number of parameters that are potentially important in determining the shape of the pattern formed. These include the viscosities of the fluids, the flow rate, the surface tension between the fluids, the permeability of the medium, and the relative ease with which the two fluids wet the medium. In this paper, we describe preliminary results of an investigation of the patterns formed by immiscible displacement in a thin porous medium in which all of these parameters are systematically varied. We find that the phenomena observed can be divided into two major categories, depending on whether or not the displacing fluid preferentially wets the medium. The wetting behavior has a major effect on the width of the individual fingers. If the displacing fluid preferentially wets the medium, then the width of a typical finger is always found to be much larger than the characteristic pore size, and to follow a scaling law that depends on the flow rate, surface tension, and permeability of the medium. However, if the displaced fluid preferentially wets the medium, then the finger widths are found to be on the same order as the pore size, essentially independent of the other parameters. Consequently, the overall shape of the patterns also depends strongly on the wetting behavior. We refer to these two cases as wetting and nonwetting, respectively, and note that in the literature on porous media they are also referred to as imbibition and drainage.[12]

Our experiments are done in a cell of adjustable dimensions, typically 30 cm long and 7 cm wide, with a gap of 0.15 cm. The cell is packed with unconsolidated glass beads to form the random porous medium. The beads are sieved so that the diameters have a variation of roughly $\pm 20\%$ about the mean, with the resultant porosity measured to be $p = 0.43$. Since the thickness of the cell is always several times the diameter of the beads, the pore geometry is three dimensional. Nevertheless, the interface does not vary appreciably across the thickness of the cell, so that the patterns themselves are two dimensional in the wetting case. This allows for simple visualization.

The experiments are performed by first filling the cell uniformly with the more viscous fluid, then injecting the less viscous fluid at constant volume flow rate Q by means of a syringe pump. Injection and collection of the fluids are done from small holes at opposite ends of one of the plates, while all the measurements are made in the center of the cell, thus avoiding end effects in the flow patterns and any initial transients in the flow. The fluid that preferentially wets the beads is water, or a water-glycerol mixture when an increase in viscosity is desired, while the nonwetting fluid is chosen from a selection of oils of various viscosities.

The inverse resistance to flow is characterized by the permeability κ defined by the relationship between the flow velocity U and pressure gradient ∇P, $U =$

$-(\kappa/\mu)\nabla P$. Here $U=Q/Ap$, where A is the cross-sectional area of the cell, and μ is the viscosity. We note that this formulation of Darcy's law differs from the usual one as we consider the true velocity rather than the superficial velocity Q/A. As a result, our permeability also differs by a factor of p from the usual one. We vary the permeability, which scales roughly as the square of the mean bead size, over two orders of magnitude, $2\times10^{-7}\leq\kappa\leq4\times10^{-5}$ cm^2. The surface tension between the two fluids γ is also measured, and can be varied by addition of a small amount of surfactant to the water.

For a fluid flowing in a porous medium, the viscous forces result in a pressure difference of order $\mu Ur/\kappa$ across a typical pore dimension r. At the interface between the two fluids, there is also a capillary pressure difference of order γ/r. The capillary number, $N_{Ca}=\mu U/\gamma$, is a dimensionless quantity which reflects the relative strengths of viscous and capillary forces. All our experiments were performed with a viscosity ratio, $M=\mu_2/\mu_1$, greater than 100, ensuring that the pressure is dropped exclusively across the more viscous fluid. This was confirmed by measurement of the pressure required to sustain a constant Q. Thus, the appropriate viscosity for N_{Ca} is μ_2.

Typically, the index of refraction of the oil closely matches that of the glass beads, while that of the water is sustantially different, leading to more light scattering from the water-coated beads, and allowing the pattern to be visualized. When the indices are similar, an absorbing dye is added to the displacing fluid for visualization.

Examples of typical patterns formed in the *wetting* case are shown in Figs. 1(a) and 1(b) for different bead sizes and $M=195$. Closer examination by use of a low-power microscope reveals that virtually all the oil is displaced by the water in the figures. We find that it is possible to define a mean finger width w which depends only on κ and N_{Ca}. We find that w decreases with decreasing κ and with increasing N_{Ca}, but is always substantially larger than the bead size and therefore larger than any characteristic length scale of the pore space. The overall shape of the pattern depends on the width of the finger compared to that of the cell. At the lowest flow rates, a single uniform finger forms, whose width is comparable to that of the cell. As N_{Ca} increases, the width and direction of the finger begin to fluctuate. As N_{Ca} increases further, the finger width decreases and tip-splitting instabilities occur as shown in Fig. 1(a). However, one branch always moves faster, while the second ultimately stops. At still higher N_{Ca}, when the finger width becomes substantially less than that of the cell, the tip-splitting instability occurs more frequently, and several fingers can coexist for considerable distances. This same behavior is observed at lower N_{Ca} when κ is reduced by use of smaller beads. An example of this, illustrating considerable tip splitting, is shown in Fig. 1(b). The boundary of the finger in the tip-splitting regime is always irregular, with roughness on length scales extending from the finger width to the bead size.

To investigate quantitatively the dependence of w on the various parameters, we digitized video images of the patterns and measured the width of each of the fingers intersected by each column of pixels in the image. From the resultant distribution of finger widths, we determined the mean width w, as well as the standard deviation, which was typically close to half the mean finger width. We also measured the total area and perimeter of the patterns, and calculated a mean width from the ratio. Both forms of analysis gave

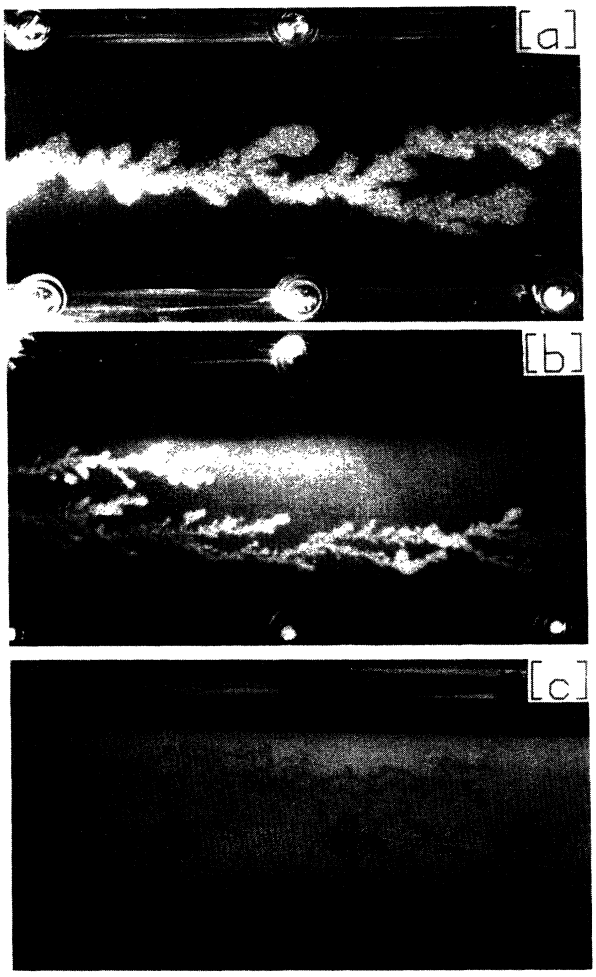

FIG. 1. (a) Wetting displacement with water (light color) displacing oil (dark). Here $d=0.5$ mm ($\kappa=2\times10^{-6}$ cm^2) and $N_{Ca}=6.9\times10^{-4}$. (b) Wetting displacement with $d=0.15$ mm ($\kappa=2\times10^{-7}$ cm^2) and $N_{Ca}=3.8\times10^{-4}$. (c) Nonwetting displacement with oil (dark) displacing water and glycerol (light). Here $d=0.5$ mm ($\kappa=2\times10^{-6}$) and $N_{Ca}=2.3\times10^{-4}$. $M\approx200$ in all cases.

similar results.

The measured values of the finger width under a wide variety of conditions in the tip-splitting regime are summarized in Fig. 2. We have normalized w by the square root of the permeability, making it dimensionless. Data taken with three different bead sizes, with κ varying over two orders of magnitude, are plotted as a function of the capillary number. To test whether N_{Ca} is a control parameter, we independently measured the dependence of w on μ, U, and γ. We have varied Q (and therefore U) by roughly two orders of magnitude, with the resultant finger widths approaching about half the cell width at the low velocities, and the cell thickness at the large velocities. The interfacial surface tension between the two fluids was varied by nearly a decade by addition of different amounts of surfactant to the water. We also varied μ_2 by more than a factor of 5, but always maintained $M > 100$. When scaled, the data points lie on a single line, to within experimental error. This verifies that N_{Ca} is indeed a control parameter, and also that the finger width scales as the pore size, rather than any cell dimension. From a least-squares fit to the data, we measure the slope to be -0.51 ± 0.1. We note that there is a broad distribution of finger widths, primarily because of the existence of the tip splitting. The number of splittings observed in each picture varies widely, leading to a concomitant variation in the measured w. We believe that this is the origin of the considerable scatter evident in the data.

In contrast, the behavior for the *nonwetting* case is markedly different, as shown in Fig. 1(c), again for $M \approx 200$. Here the finger width is comparable to the characteristic length scale of the pore spaces and is roughly independent of N_{Ca}. Visualization is more difficult because the displacing fluid does not fill the full

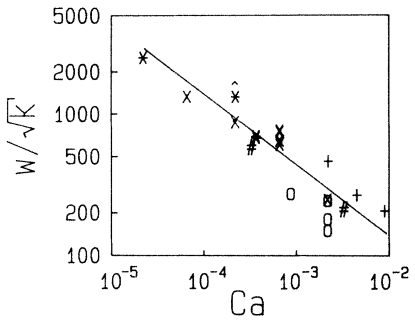

FIG. 2. Normalized finger width ($w/\kappa^{1/2}$) vs N_{Ca} for wetting displacement. The data points refer to asterisks, $d = 0.15$ mm; crosses, $d = 0.5$ mm; circles, $d = 1.7$ mm, all with N_{Ca} varied by changing Q; plusses, $d = 0.5$ mm, $Q = 1.5$ ml/min, with N_{Ca} varied by changing γ; number signs, $d = 0.5$ mm, with N_{Ca} varied by changing μ_2; caret, $d = 0.15$ mm, cell width decreased by a factor of 2. The solid line is a least-squares fit with a slope of -0.51.

depth of the cell. The patterns are more disordered in appearance, and again exhibit tip splittings, whose frequency increases with N_{Ca}. While the width of the fingers does not depend on N_{Ca}, the number of fingers which coexist across the width of the cell increases with N_{Ca}.

It is instructive to compare our observations to those obtained for immiscible displacement in other geometries. The nonwetting case corresponds rather closely to the behavior observed in two-dimensional micromodel experiments,[11-13] where the fluid displacement is well described by invasion percolation[14] at low N_{Ca}, and by analogy to diffusion-limited aggregation at high Ca. In both cases, the smallest length scale of the pattern is the pore size. The patterns formed in our cell are consistent with this picture.

In contrast, the patterns formed in the wetting case bear some resemblence to those formed in the traditional Hele-Shaw geometry. In both cases, N_{Ca} is a control parameter and the finger width is much larger than the smallest characteristic length. In the Hele-Shaw cell at low N_{Ca}, a single stable finger is formed, whose width and shape are both determined by the cell geometry, with the highly nonlocal nature of the flow causing the walls to play a crucial role.[2] Thus the finger width is related to the cell width, and does not scale with $N_{Ca}^{-1/2}$. As N_{Ca} increases, fluctuations in the permability can lead to a tip-splitting instability resulting in patterns that are qualitatively similar[15-17] to those found here.

In the porous medium at very low Q, we also observe a single uniform finger whose width is comparable to the cell size. After the onset of tip scattering, the individual finger widths are solely determined by κ and N_{Ca} and not the cell width. This was confirmed by repeating one run in a cell whose width was decreased by a factor of 2, and observing that w was unchanged. The behavior is quite different from that of the stable finger in Hele-Shaw flow, but may resemble that in the tip-splitting regime. Our observations suggest that it might be interesting to analyze the tip-splitting fingers in a Hele-Shaw cell to determine whether the width exhibits a scaling behavior similar to that found here.

The form of the observed scaling behavior might be explained on physical grounds if we assume that the instability occurs when the viscous and capillary pressure drops are comparable on the length scale of the finger width. This would result in w scaling as $(\kappa/N_{Ca})^{1/2}$. Similar results are obtained from a linear stability analysis[8] for the fastest-growing wavelength. Though these *seem* to account for the observed scaling, the analyses assume that the relevant interfacial tension between the two fluids is determined by the macroscopic curvature at the finger tip. Since the interface must locally satisfy the correct boundary conditions and so have the appropriate contact angle with

the pore walls, it is quite rough on the scale of a pore size. Thus it is not clear to what extent the gross curvature at the finger tip determines the interfacial tension. The analyses also drastically underestimate the characteristic length, and can be made to agree with experiment only by replacement of the interfacial surface tension by an empirically determined effective surface tension that depends on the wettability of the medium,[9] but is always substantially larger than γ.

The large magnitude of the finger width in the wetting case and its scaling with N_{Ca} are still essentially unexplained. The key to a more rigorous picture of the instability is a better understanding of the basic physics of the flow at the interface itself. This is most clearly emphasized by our observation that the patterns produced under otherwise identical conditions are dramatically different if the relative wettability of the fluids is reversed.

We conclude by noting that our experiments show the validity of the diffusion-limited-aggregation model[10,11] in describing viscous fingering to be highly restricted since the effects of wettability and capillary number are not included. It works for the nonwetting displacement where the smallest length scale is fixed by the pore size and is much smaller than the cell width. In contrast, the shortest length scale for wetting displacement is larger and depends on many parameters. Indeed, we have never observed an unambiguously fractal pattern in the wetting case. Therefore, the analogy to diffusion-limited aggregation, while appealing because of its elegance and simplicity, must be used with great caution in describing viscous fingering patterns in porous media.

We acknowledge useful discussions with Eric Herbolzheimer, Fyl Pincus, Len Schwartz, and Eric Siggia. The work of two of us (A. D. and J. P. G.) was supported by National Science Foundation Low Temperature Physics Grant No. DMR-8503543.

[1]L. P. Kadanoff, D. Bensimon, S. Liang, B. Shraiman, and C. Tang, Rev. Mod. Phys. (to be published).

[2]B. I. Shraiman, Phys. Rev. Lett. **56**, 2028 (1986); D. C. Hong and J. S. Langer, Phys. Rev. Lett. **56**, 2032 (1986); R. Combescot, T. Dombre, V. Hakim, and Y. Pomeau, Phys. Rev. Lett. **56**, 2036 (1986).

[3]D. Kessler and H. Levine, Phys. Rev. A **33**, 2621, 2634 (1986).

[4]P. Tabeling and A. Libchaber, Phys. Rev. A **33**, 794 (1986); P. Tabeling, G. Zocchi, and A. Libchaber, unpublished.

[5]J. Maher, Phys. Rev. Lett. **54**, 1498 (1985).

[6]C. W. Park and G. M. Homsy, J. Fluid Mech. **139**, 291 (1984); C. W. Park, S. Gorell, and G. M. Homsy, J. Fluid Mech. **141**, 275 (1984).

[7]G. Daccord, J. Nittmann, and H. E. Stanley, Phys. Rev. Lett. **56**, 336 (1986).

[8]R. L. Chuoke, P. van Meurs, and C. van der Poel, Trans. AIME (Am. Inst. Min. Metall. Pet. Eng.) **216**, 188 (1959).

[9]E. Peters and D. Flock, Soc. Pet. Eng. J. **21**, 249 (1981).

[10]L. Paterson, Phys. Rev. Lett. **52**, 1621 (1984); L. Paterson, V. Hornof, and G. Neale, Rev. Inst. Fr. Pet. **39**, 517 (1984) and Soc. Pet. Eng. J. **24**, 325 (1984).

[11]K. Maloy, J. Feder, and T. Jossang, Phys. Rev. Lett. **55**, 2688 (1985).

[12]R. Lenormand and C. Zarcone, Phys. Rev. Lett. **54**, 2226 (1985), and J. Fluid Mech. **135**, 337 (1983), and in Proceedings of the 59th Annual Technical Conference of the Society of Petroleum Engineers of AIME, 1984, Report No. 13264, unpublished.

[13]J.-D. Chen and D. Wilkinson, Phys. Rev. Lett. **55**, 1892 (1985).

[14]D. Wilkinson and J. F. Willemsen, J. Phys. A **16**, 3365 (1983); D. Wilkinson, Phys. Rev. A **30**, 520 (1984).

[15]C. W. Park and G. M. Homsy, Phys. Fluids **28**, 1583 (1985).

[16]A. J. DeGregoria and L. W. Schwartz, Phys. Fluids **28**, 2313 (1985).

[17]E. Ben-Jacob, R. Godbey, N. D. Goldenfeld, J. Koplik, H. Levine, T. Meuller, and L. M. Sander, Phys. Rev. Lett. **55**, 1315 (1985).

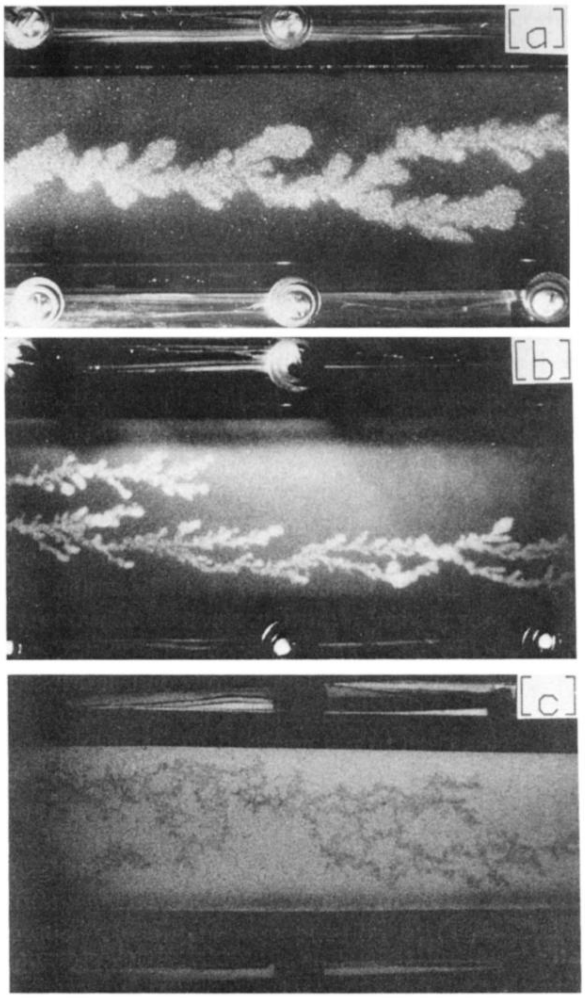

FIG. 1. (a) Wetting displacement with water (light color) displacing oil (dark). Here $d=0.5$ mm ($\kappa=2\times10^{-6}$ cm^2) and $N_{Ca}=6.9\times10^{-4}$. (b) Wetting displacement with $d=0.15$ mm ($\kappa=2\times10^{-7}$ cm^2) and $N_{Ca}=3.8\times10^{-4}$. (c) Nonwetting displacement with oil (dark) displacing water and glycerol (light). Here $d=0.5$ mm ($\kappa=2\times10^{-6}$) and $N_{Ca}=2.3\times10^{-4}$. $M\approx200$ in all cases.